Elastically controlled manipulation of the magnetic order parameter and the metal-insulator transition in a manganite thin film

Surendra Singh, M. R. Fitzsimmons, T. Lookman, H. Jeen, and A. Biswas

Phys. Rev. B **90**, 060407 — Published 22 August 2014

DOI: 10.1103/PhysRevB.90.060407

Elastically controlled manipulation of the magnetic order parameter and the metal-insulator-transition of a manganite thin film

Surendra Singh,[1,*] M. R. Fitzsimmons,[2] T. Lookman,[2] H. Jeen[3,4] and A. Biswas[3]

[1] Solid State Physics Division, Bhabha Atomic Research Center, Mumbai 400085, India

[2] Los Alamos National Laboratory, Los Alamos, NM 87545, USA

[3]Department of Physics, University of Florida, Gainesville, FL 32611, USA

[4]Department of Physics, Pusan National University, Busan 609-735, Korea

*Email: surendra@barc.gov.in

Abstract: We measured the temperature dependence of the saturation magnetization (M_s) of a $(La_{1-x}Pr_x)_{1-y}Ca_yMnO_3$ (x ~ 0.60, y ~ 0.33) film as a function of applied bending stress. Stress producing a compressive strain of -0.01% along the magnetic easy axis increased the Curie temperature by ~6 K and the metal-insulator-transition by ~4 K. Regardless of whether or not stress is applied to the film, magnetic ordering occurs at temperatures significantly higher than the metal-insulator-transition temperature. The magnetization of the sample at the temperature of the metal-insulator transition is approximately the site percolation threshold for a two-dimensional spin lattice.

PACS numbers: 75.70.Cn; 75.47.Lx; 75.25.-j

Hole doped manganites are strongly correlated oxides that show a large variety of magnetic and electronic phases due to competing interactions between the orbital, charge, lattice and spin degrees of freedom.[1,2,3] The competing interactions lead to complex behavior such as colossal magnetoresistance (CMR) often accompanied with metal-to-insulator transitions (MIT).[4,5,6,7] Competition between the interactions can be influenced by electric fields,[8,9] magnetic field,[6] light,[10] stress/strain,[3,11,12,13,14] disorder.[14] Among these parameters, stress/strain is ubiquitous in thin films and devices, and can significantly affect the properties of manganite thin films.[3,11,12,13,15,16,17,18] Recently, we observed a strong influence of applied bending stress on the saturation magnetization, M_s, at the MIT, T_{MI}, of a manganite film.[19] Namely, compressive stress increases M_s and T_{MI}. Curiously, theoretical guidance for a relation between M_s and stress is still lacking. On the other hand, Millis *et al*.,[17] proposed an analytical model to describe the effects of biaxial strain on the Curie temperature (T_c) of CMR manganites. For example, 1% biaxial strain can cause a 10% shift of the T_c.

Several studies have reported that films exhibit unique electronic and magnetic properties that depend upon film thickness[12] or choice of growth substrate.[13] Often these differences are attributed to differences of epitaxial strain, though epitaxial strain and the extent of the strain field into the film are two of many structural features affected by film thickness and choice of substrate. Some studies have used structural phase transformation[20] or the piezoelectric property[21] of a substrate to apply stress to a film and still yielded contradictory results. Piezoelectric studies are further complicated by the competing influences of strain and charge accumulation at the film/piezoelectric interface. The techniques also impose specific requirements for single crystal films limiting their use to only films that can be epitaxially grown on substrates exhibiting piezoelectric response or structural transformations. Thus, the *exclusive*

influence of elastic stress on the Curie temperature of a manganite thin film has not been systematically, nor quantitatively studied. Our results qualitatively agree with the prediction of Millis *et al.*[17]; however the experimental observation and the theoretical prediction are quantitatively inconsistent.

In manganites, mesoscopic phase coexistence associated with first order phase transition is believed to be related to the nonstandard percolative nature of the MIT,[1,2,3,4,5,6,7] which remains a long-standing controversial problem. In fact there is disagreement about the nature of MIT in manganites with groups claiming it to be a Mott insulator[22] while other groups claiming it not to be a pure Mott insulator but rather have major contribution of structural distortion in the form of Jahn-Teller distortion, which also favors magnetization in manganites.[4,18] The ambiguity reopens the fundamental question of what the origin of the MIT and whether magnetic transition leads to MIT or vice versa.

Here, we report the influence of applied elastic bending stress on the magnetic ordering temperature of a single crystalline $(La_{1-x}Pr_x)_{1-y}Ca_yMnO_3$ ($x \sim 0.60$, $y \sim 0.33$) (LPCMO) film. Simultaneous measurements of polarized neutron reflectivity (PNR) data and resistance data from the LPCMO film as a function of temperature demonstrate that magnetic ordering occurs at significantly higher temperatures (~ 30 K) than the MIT, well within the insulating phase. A significant increase of both the MIT and T_c with small (-0.01%) compressive strain was observed, which suggest that changes of elastic strain alone are sufficient to affect the electronic properties and magnetic ordering in LPCMO thin films. The magnetization of the sample at the temperature of the metal-insulator transition is consistent with the site percolation threshold for a two-dimensional system.

A 20-nm-thick LPCMO film was epitaxially grown on a 1cm by 1 cm (110) $NdGaO_3$ (NGO) substrate in the step-flow-growth-mode using pulsed KrF laser (248 nm) deposition (PLD).[23] During growth, the substrate temperature was 1053 K, O_2 partial pressure was 17.33 Pa, laser fluence was 0.5 J/cm^2, and the repetition rate of the pulsed laser was 5 Hz. The thickness of the substrate was 0.25 mm.

Bending stress was applied parallel to the magnetic easy axis of the sample (parallel to $[1\bar{1}0]$ NGO)[23,24] using a four point mechanical jig, which applied stress uniformly over the lateral dimensions of a large sample.[19] The lattice mismatch between bulk LPCMO and NGO is about 0.26% and 0.49% along [001] and $[1\bar{1}0]$ NGO, respectively.[23] In spite of considerable difference in epitaxial strain along two perpendicular in-plane directions we didn't observe any change in MIT along these orthogonal directions. Since we are examining one sample as a function of *applied bending stress*, the so-called epi-strain resulting from lattice mismatch is not affected by our experiment. The sample was cooled or warmed in the 6 kOe field (applied along the easy axis) at a rate of 0.40±0.05 K/min. The 6 kOe field is an order of magnitude larger than the field required saturating the magnetization.[24] The bending strain of the film was measured using[25,26] : $\varepsilon = \frac{t_s}{r}$, where t_s and r are the thickness of substrate and the radius of curvature of film, respectively. The radius of curvature of the sample was measured with a laser.[27] The electrical transport (resistance), R(T), measurements for the sample with compressive strain (ε = - 0.01%) and ε = 0% (without applied stress) at a field of 6 kOe are shown in Fig. 1(a). The maximum of dR/dT on warming curves yields the metal-insulator transition temperature T_{MI} = 101.4 K without applied stress and 105.4 K with applied compressive stress. T_{MI} represents the temperature at which percolation of the metallic phase is detected in a film with centimeter lateral dimensions. Small compressive bending stress (i.e. $\varepsilon \sim$ -0.01%) induces a positive shift of

T_{MI} by ~ 4 K (~ 4% increase in T_{MI}) [Fig. 1(a)]. Thus the change in MIT with applied compressive stress indicates that compressive strain field affects percolation.

In order to probe the depth dependent structure and magnetization of the film, we carried out specular X-ray reflectivity (XRR) and PNR measurements.[19,24,28,29] The specular reflectivity, $\mathfrak{R}$, of the sample was measured as a function of wave vector transfer, $Q = 4\pi \sin\theta/\lambda$ (where, θ is angle of incidence and λ is the x-ray or neutron wavelength). The reflectivity is qualitatively related to the Fourier transform of the scattering length density (SLD) depth profile $\rho(z)$, averaged over the whole sample area. In case of PNR, $\rho(z)$ consists of nuclear and magnetic SLDs such that $\rho^{\pm}(z) = \rho_n(z) \pm CM_s(z)$, where C = 2.91×10^{-9} Å^{-2}(kA/m)$^{-1}$ and M_s(z) is the saturation magnetization (in kA/m) depth profile.[28] The +(-) sign denotes neutron beam polarization along (opposite to) the applied field. $\rho_n(z)$ and M_s(z) can be inferred from $\mathfrak{R}^{\pm}(Q)$ often with nm+ resolution. The reflectivity data were normalized to the Fresnel reflectivity[28] ($\mathfrak{R}_F = \frac{16\pi^2}{Q^4}$).

Fig. 1 (b) shows the XRR measurements from the sample. The XRR guides modeling of the film's chemical (or nuclear) structure, *e.g.,* film thickness, roughness, *etc.* Previously, scanning transmission electron energy-loss spectroscopy (EELS) microscopy[19,24] found the composition of an identically prepared film to be $(La_{1-x}Pr_x)_{1-y}Ca_yMnO_3$(x ~ 0.55, y ~ 0.23) averaged over the entire thickness of the sample. The average composition, however, does not adequately represent the significant variation of the chemical depth profile. Using EELS measurements as a guide, the XRR was modeled using three chemically distinct regions (surface (I), bulk-film (II) and film-substrate (III) regions) as shown in Fig. 1(c). [19,24]

The PNR measurements (Fig. 2) were carried out using the Asterix spectrometer at LANSCE.[28] The schematic in the inset of Fig. 2 (a) shows the bending of the film is done along an axis perpendicular to the neutron (n) beam, so the rocking width of the sample is not affected in the plane of specular reflection. Figs. 2(a) and (b) show $\mathcal{R}^{\pm}(Q)$ in the absence of compressive strain at 170 K (in the non-magnetic phase) and 20 K, respectively. At 170 K, the reflectivities measured with and without applied stress were statistically the same. The inset of Fig. 2(b) shows $\mathcal{R}^{\pm}(Q)$ at 20 K for the compressive strain condition ($\varepsilon \sim$ -0.01%).

Reflectivity data were analyzed using the dynamical method of Parratt.[19,24,28] The nuclear SLD shown as the solid (black) curve in Fig 2(c) is an optimal fit to $\mathcal{R}^{\pm}(Q)$ [solid (black) curves in Figs 2(a)] at 170 K. The three regions with different nuclear (chemical) SLD's are represented as I (surface), II (bulk-film) and III (film-substrate interface) in Fig. 2(c). Next, the nuclear SLD was fixed and then *only* the three values of M_s corresponding to Regions I, II and III were optimized to the PNR data taken at 20 K. Fig. 1(d) shows $M_s(z)$, as the solid (black, $\varepsilon = 0$) and dash (blue, ε = -0.01%) depth profiles yielding the curves in Fig. 2(b). The fits assumed the same roughness for the magnetic and nuclear interfaces. Because the fit was already very satisfactory, further adjustable parameters, *e.g.* different values for magnetic and nuclear roughness, are not warranted. Regardless of variation of the chemical composition across the film's thickness, M_s is larger for the strained film compared to the unstrained film. This result is consistent with the previous study of an identically prepared sample.[19]

We next investigated the *temperature dependence* of the M_s for conditions without and with compressive strain. PNR data were collected for a range of Q extending to 0.032 Å^{-1} in order to maximize the number (thirty-two) of temperature measurements. Fig. 3**(a)** and (**b)** show the PNR data (symbols) as well as corresponding fit (solid lines) to data for few temperatures above MIT

for conditions without and with compressive strain, respectively. Fitting only M_s, we obtained the results shown in Fig. 4 for Region II. The resistance measurements on warming cycle of the sample for the two states of strain are superimposed on the $M_s(T)$ results in Fig. 4(**a**). $M_s(T)$ near the magnetic ordering temperature is shown in Fig. 4(**b**).

Because M_s(T) exhibits thermal hysteresis (see Fig. 4 in Ref. 24) consistent with a first order transition, a fit of M_s(T) to extract a power law dependence of the order parameter with temperature is not correct. To estimate values of T_c, we fitted M_s to a line in the temperature region between 120 K and 130 K. Extrapolating the line to $M_s = 0$ yields an estimate of T_c. We obtained T_c of ~134.1 K and 140.1 K for sample without and with application of bending stress. The T_c is ~30 K greater than the MIT. Since the transport measurements were made during the neutron experiment, the difference between the T_{MI} and T_c cannot be due to errors in thermometry. For the film bulk, the shift of T_c with -0.01% (compressive) strain is ~6 K (~ 4.5% increases in T_c). Thus, compressive strain promotes magnetism in LPCMO films to higher temperatures compared to the absence of applied stress. Similar (~ 4 %) increases of T_c and the MIT with an applied compressive strain of ~ -0.01% is circumstantial evidence for an intimate relationship between the magnetic and metallic phases. The observed increase (~ 4 %) in T_c with small applied bending compressive stress (~ -0.01%) is extraordinarily higher then theoretically predicted value (i.e. 1% strain changes T_c by 10%) for biaxial strain.[17]

A second remarkable finding is $T_c >> T_{MI}$. At 120 K the sample is insulating and yet retains ~60% of its 20 K saturation magnetization, i.e., $M_s(T_{MI})/M_s$(20 K) ~ 0.6 (Fig. 4(**a**)). These data lead us to confirm that magnetic ordering occurs in the film at temperatures much higher than the MIT (for a sample with effectively infinite lateral dimensions) whether or not stress is applied to the film. One can ask whether the value, 0.6, of M_s at T_{MI} relative to M_s at 20 K has significance.

A comparison of TEM and Lorentz microscopies[6] suggested that in *bulk* LPCMO the metallic and ferromagnetic phases were from the same parts of the sample. If we assume the metallic and ferromagnetic phases are from the same parts of our LPCMO film then 60% of our film must be metallic at T_{MI} (because 60% of the sample is ferromagnetic at T_{MI} compared to 100% at 20 K). The metallic fraction of the sample yielding (electronic) percolation—the percolation threshold—is consistent with site percolation thresholds for *two-dimensional* lattices which range from 0.5 (triangular lattice), [30] 0.59 (square lattice)[31] to 0.7 (honeycomb lattice), [32,33] or bond percolation thresholds varying between 0.35 and 0.65.[33] Percolation thresholds for three-dimensional lattices[34] which are considerably smaller than thresholds for two-dimensional lattices. The assumption that ferromagnetic and metallic phases are co-located in the LPCMO film is challenged by the notion that a 20nm thick film is representative of a two-dimensional system.

In summary, we found that bending stress producing 0.01% compressive strain increases the Curie temperature of the LPCMO film bulk by ~6 K—considerably larger than suggested by Millis *et al.*[17] Compressive strain also increases the metal-insulator-transition temperature by nearly the same amount (~4 K) as T_c. Thus, compressive elastic strain favors the magnetic and metallic phases. Most importantly, the film retains significant magnetic order ~30 K above the metal-insulator transition. We conclude that magnetic ordering is not caused by the metal-insulator transition rather magnetic ordering first occurs at higher temperature. When the magnetic ordering as measured by the ratio of saturation magnetization normalized to the 20 K value, i.e., $M_s(T)/M_s($20 K$)$, is less than ~0.6, the film's resistance measured over macroscopic dimensions changes from metallic to insulating. The value of ~0.6 is consistent with the site percolation threshold for two-dimensional spin lattices, if the magnetic phase is also metallic (a

supposition supported by the similarity of increases of T_c and the MIT with compressive strain). Our experimental technique further enables studies of functional materials in which only the conjugate field of elastic stress is perturbed. Results from such studies should be most amenable for comparison to theoretical predictions from a variety of interesting systems such as multiferroics, piezeomagnets, and ferrotoroids.

This work was supported by the Office of Basic Energy Science (BES), U.S. Department of Energy (DOE), BES-DMS funded by the DOE's Office of BES, the National Science Foundation (DMR-0804452) (HJ and AB). Discussions with Profs. S.K. Sinha and Ivan K. Schuller and Drs. S. Guenon, G. Ramírez, T. Saerbeck are gratefully acknowledged. Los Alamos National Laboratory is operated by Los Alamos National Security LLC under DOE Contract DE-AC52-06NA25396.

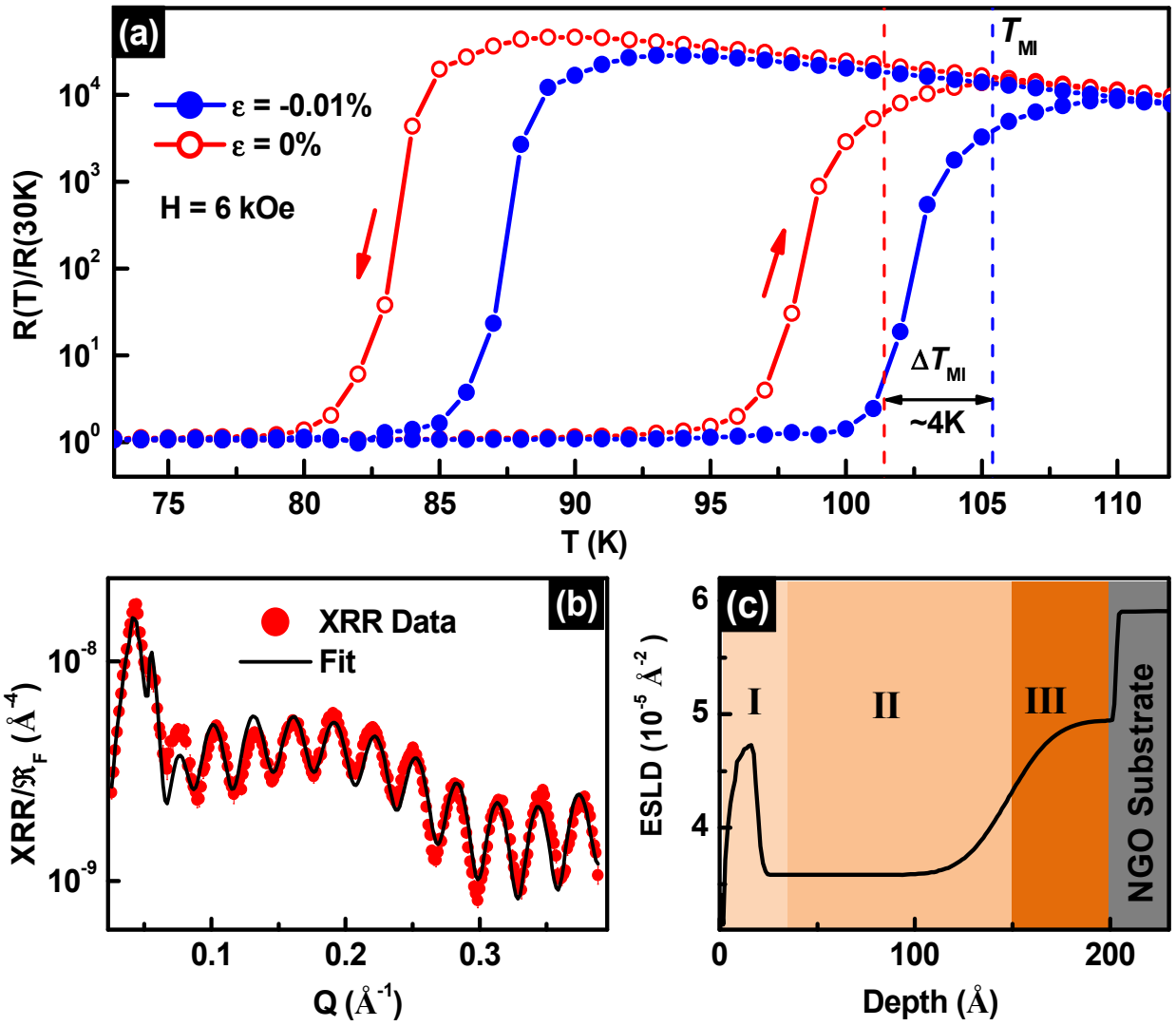

Fig. 1: **(a)** Transport measurements of the film at different applied bending stress/strain, compressive (●) and no strain (⊖). **(b)** X-ray reflectivity (XRR) data normalized to the Fresnel reflectivity (symbols) and corresponding fits (solid line) to data. **(c)** electron scattering length density (ESLD) depth profile which yielded best fit to XRR data.

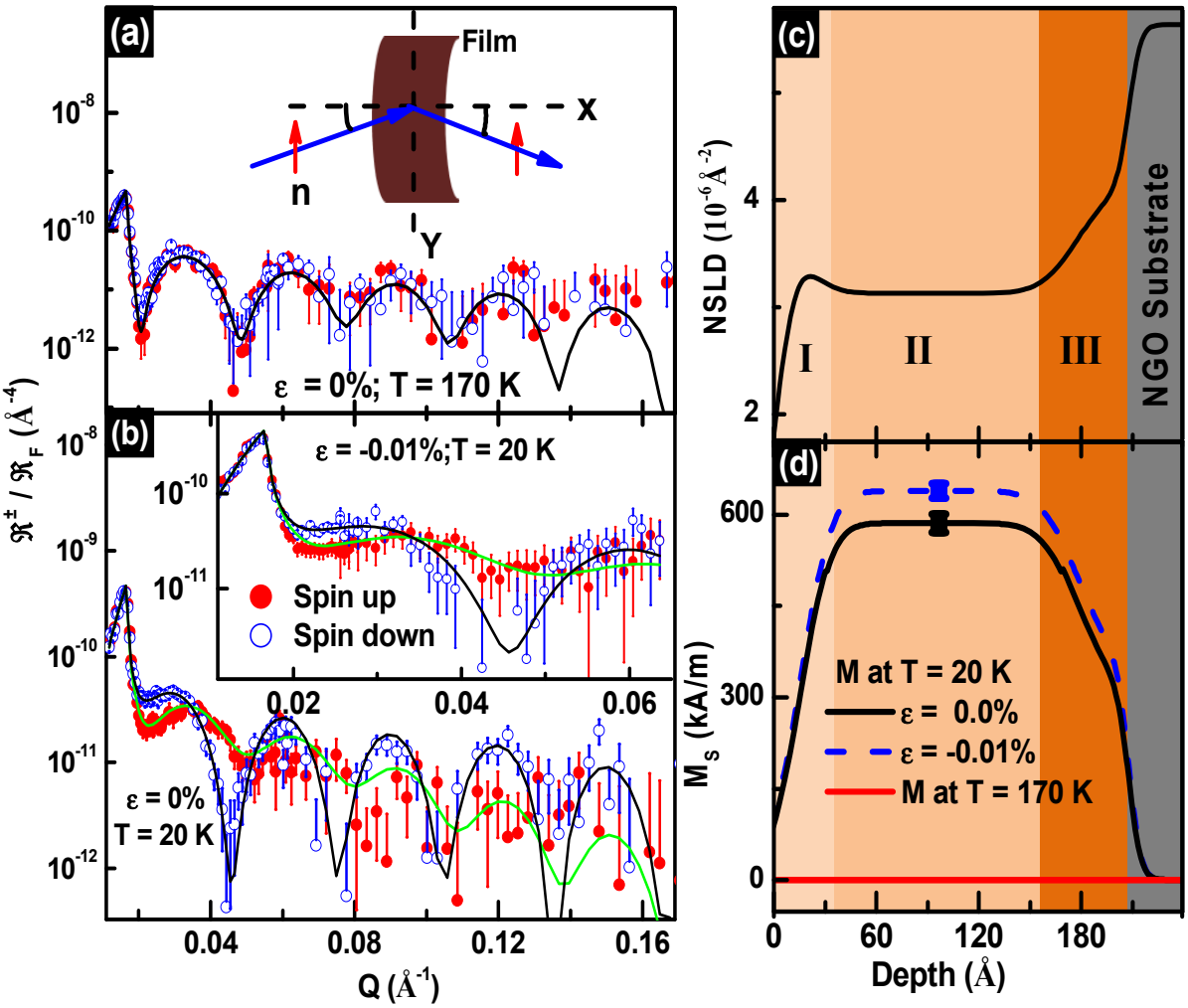

Fig. 2: PNR data normalized to the Fresnel reflectivity (symbols) from LPCMO film without applied stress at T = 170 K (a) and 20 K (b). Inset of (a) shows the schematic of axis of bending of the film and neutron reflectivity measurement. Inset of (b) shows the PNR data from the LPCMO film at T = 20 K with applied compressive stress producing ε = -0.01%. (c) Nuclear scattering length density depth profile (NSLD) (d) and saturation magnetization depth profiles, which yield the solid curves (fit for PNR data, green/black) in (a) and (b).

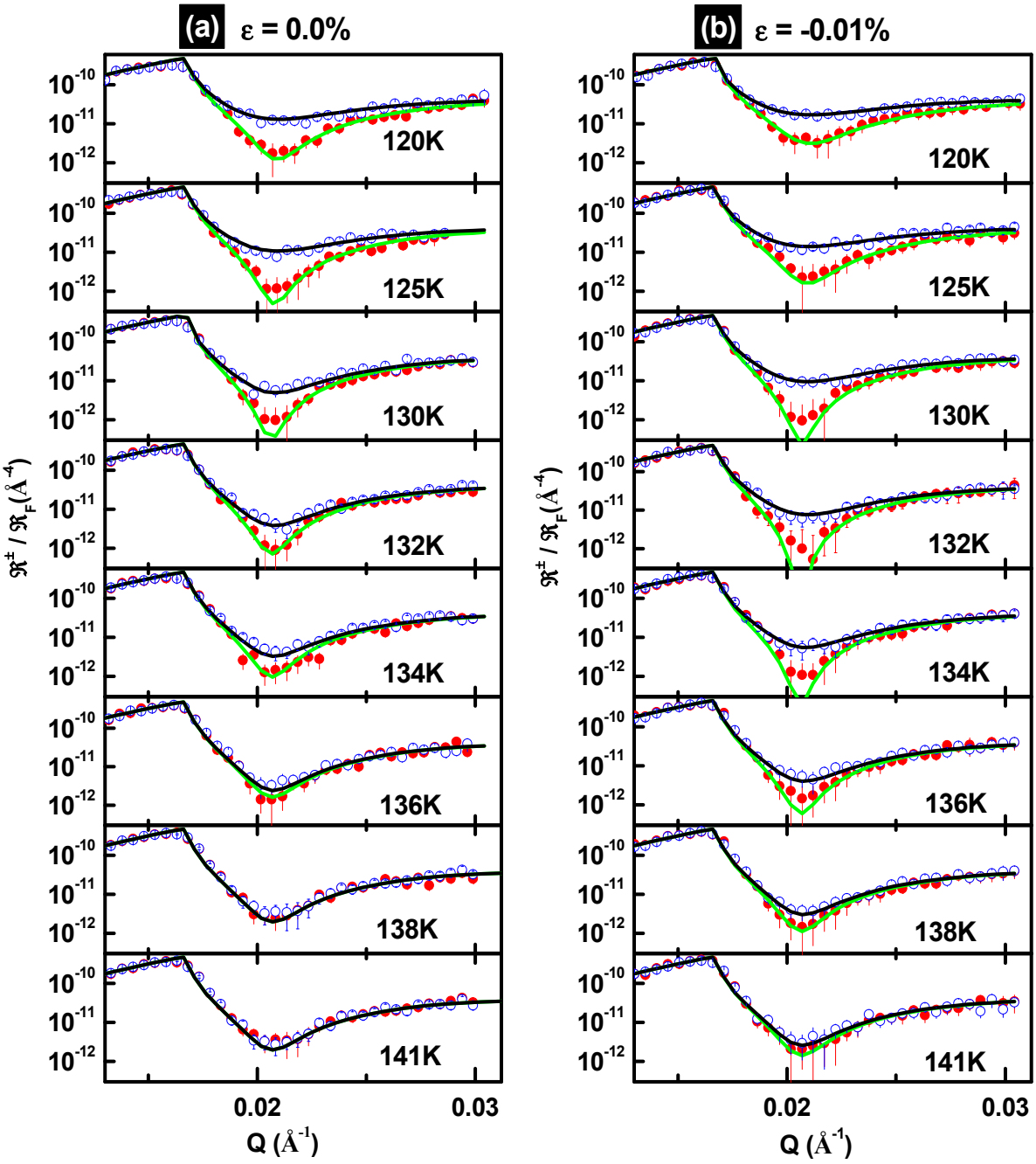

Fig. 3: PNR data normalized to the Fresnel reflectivity (symbols) and corresponding fits (solid curves) to data at different temperatures above MIT from sample, without (a) and with (b) applied stress.

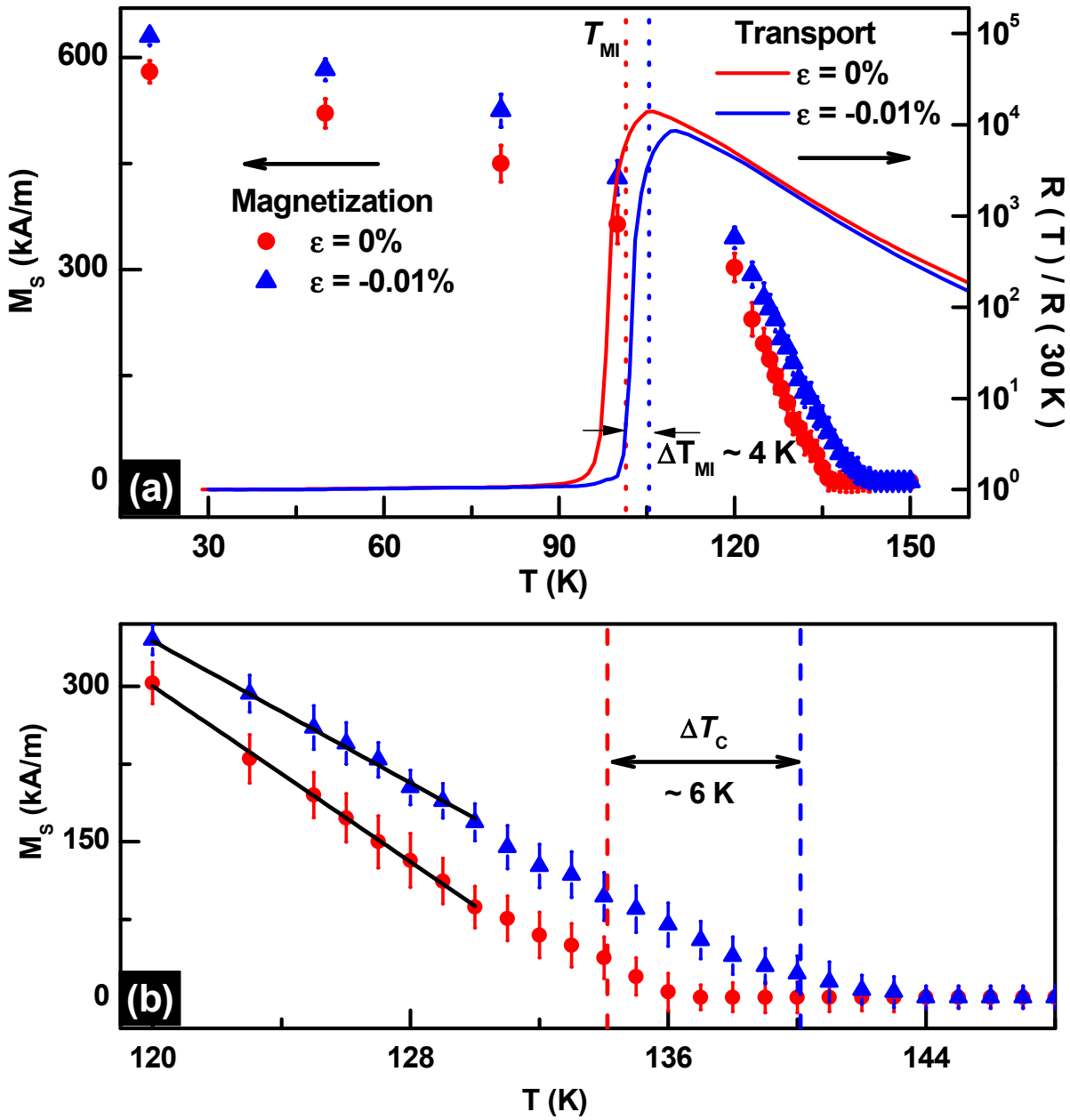

Fig. 4 (a) $M_s(T)$ obtained from the polarized neutron reflectivity of the LPCMO film without(●) and with (▲) applied bending stress while warming from low temperature. Superimposed is the resistance of the sample measured during the neutron experiment without (red) and with (blue) applied bending stress. The dotted lines correspond to the metal-insulator-transitions during warming for the two states of stress. (b) Shows the $M_s(T)$ close to the ordering temperature. Extrapolation of linear fits of $M_s(T)$ to $M_s = 0$ yields estimates for T_c.

[1] A. J. Millis, Nature **392**, 147 (1998).

[2] N. D. Mathur and P. B. Littlewood, Physics Today **56,** 25 (2003).

[3] K. H. Ahn, T. Lookman, and A. R. Bishop, Nature **428**, 401 (2004).

[4] E. Dagotto, *Nanoscale Phase Separation in Manganites* (Springer-Verlag, Heidelberg, 2002).

[5] S. Jin, T.H. Tiefel, M. mcCormack, R.A. Fastnacht, R. Ramesh, L.H. Chen, Science **264**, 413 (1994).

[6] M. Uehara, S. Mori, C. H. Chen, and S.-W. Cheong, Nature **399**, 560 (1999).

[7]M. Bibes, Ll. Balcells, S. Valencia, J. Fontcuberta, M. Wojcik, E. Jedryka, and S. Nadolski, Phys. Rev. Lett. **87**, 067210 (2001).

[8] H. Sakai and Y. Tokura, Appl. Phys. Lett. **92,** 102514 (2008).

[9] B. T. Xie, Y. G. Zhao, and C. M. Xiong, Appl. Phys. Lett. **93,** 072112 (2008).

[10]M. Rini, R. Tobey, N. Dean, J. Itatani, Y. Tomioka, Y. Tokura, R. W. Schoenlein & A. Cavalleri, Nature **449,** 72 (2007).

[11] T. Z. Ward, J. D. Budai, Z. Gai, J. Z. Tischler, L. Yin, and J. Shen, Nat. Phys. **5**, 885 (2009).

[12]X. J. Chen, H.-U. Habermeier, H. Zhang, G. Gu, M. Varela, J. Santamaria, and C. C. Almasan, Phys. Rev. B **72**, 104403 (2005).

[13]F. H. Zhang, Z. Huang, G. Y. Gao, P. F. Chen, L. F. Wang, X. L. Tan, and W. B. Wu, Appl. Phys. Lett. **96**, 62507, (2010).

[14]E. Dagotto, Science **309**, 257-262 (2005).

[15]Y. Q. Zhang, Z. D. Zhang, and J. Aarts, Phys. Rev. B **79,** 224422 (2009).

[16]A. Sadoc, B. Mercey, C. Simon, D. Grebille, W. Prellier, and M.-B. Lepetit, Phys. Rev. Lett. **104,** 046804 (2010).

[17]A. J. Millis, T. Darling, and A. Migliori, J. Appl. Phys. **83**, 1588 (1998);

[18]C.A. Perroni, V. Cataudella, G. De Filippis, G. Iadonisi, V. Marigliano Ramaglia, and F. Ventriglia, Phys. Rev. B **68**, 224424 (2003).

[19]S. Singh, M. R. Fitzsimmons, T. Lookman, H. Jeen, A. Biswas, M. A. Roldan, and M. Varela, Phys. Rev. B **85**, 214440 (2012).

[20]M. K. Lee, T. K. Nath, C. B. Eom, M. C. Smoak, and F. Tsui, Appl. Phys. Lett. 77, 3547 (2000).

[21]C. Thiele, K. Dörr, S. Fähler, L. Schultz, D. C. Meyer, A. A. Levin, and P. Paufler, Appl. Phys. Lett. 87, 262502 (2005).

[22]I. Loa, P. Adler, A. Grzechnik, K. Syassen, U. Schwarz, M. Hanfland, G. Kh. Rozenberg, P. Gorodetsky, and M. P. Pasternak, Phys. Rev. Lett. **87,** 125501 (2001).

[23]H. Jeen and A. Biswas, Phys. Rev. B **83**, 064408 (2011).

[24]S. Singh, M. R. Fitzsimmons, T. Lookman, J. D. Thompson, H. Jeen, A. Biswas, M. A. Roldan, and M. Varela, Phys. Rev. Lett. **108**, 077207 (2012).

[25]A. Misra, & M. Nastasi, *Engineering Thin Films and Nanostructures with Ion Beams*, Chap. 7, pp. 319 (CRC Press, 2005).

[26]H. Kato, Y. Tottori, K. Sasaki, Experimental Mechanics **54**, 489 (2014).

[27]Y. T. Im, S. T. Choi, T. S. Park, & J. H. Kim, J. Mech. Sci. Tech. **18**, 12 (2004).

[28]M. R. Fitzsimmons and C. Majkrzak, *Modern Techniques for Characterizing Magnetic Materials* (Springer, New York, 2005), Chap. 3, pp. 107–155.

[29]S. Singh, A. Singh, M. R. Fitzsimmons, S. Samanta, C. L. Prajapat, S. Basu and D. K. Aswal, J. Phys. Chem. C **118**, 4072 (2014).

[30]M. E. J. Newman and R. M. Ziff, Phys. Rev. Lett. **85**, 4104 (200).

[31]K. Shida, R. Sahara, H. Mizuseki and Y. Kawazoe, Mater. Trans. **53**, 1301 (2012).

[32]Z.V. Djordjevic, H. E. Stanley and A. Margolina, J. Phys. A: Math. Gen **15**, L405 (1982)

[33]M.F. Sykes and J.W. Essam, J. of Math. Phys. **5**, 1117 (1964).

[34]M.A. Torija, M. Sharma, J. Gazquez, M. Varela, C. He,J. Schmitt, J. A. Borchers, M. Laver, S. El-Khatib, and C. Leighton, Adv. Mater. **23**, 2711 (2011).